Stoch Environ Res Risk Assess (2006) 21: 159–173
DOI 10.1007/s00477-006-0053-6

ORIGINAL PAPER

A. Chaudhuri · M. Sekhar

Stochastic modeling of solute transport in 3-D heterogeneous porous media with random source condition

Published online: 14 April 2006

Abstract During probabilistic analysis of flow and transport in porous media, the uncertainty due to spatial heterogeneity of governing parameters are often taken into account. The randomness in the source conditions also play a major role on the stochastic behavior in distribution of the dependent variable. The present paper is focused on studying the effect of both uncertainty in the governing system parameters as well as the input source conditions. Under such circumstances, a method is proposed which combines with stochastic finite element method (SFEM) and is illustrated for probabilistic analysis of concentration distribution in a 3-D heterogeneous porous media under the influence of random source condition. In the first step SFEM used for probabilistic solution due to spatial heterogeneity of governing parameters for a unit source pulse. Further, the results from the unit source pulse case have been used for the analysis of multiple pulse case using the numerical convolution when the source condition is a random process. The source condition is modeled as a discrete release of random amount of masses at fixed intervals of time. The mean and standard deviation of concentration is compared for the deterministic and the stochastic system scenarios as well as for different values of system parameters. The effect of uncertainty of source condition is also demonstrated in terms of mean and standard deviation of concentration at various locations in the domain.

Keywords Solute transport · Porous media · Heterogeneity · Random source · Stochastic FEM

A. Chaudhuri · M. Sekhar (✉)
Department of Civil Engineering, Indian Institute of Science, Bangalore 560012, India
E-mail: abhijit@civil.iisc.ernet.in
E-mail: muddu@civil.iisc.ernet.in

1 Introduction

The uncertainty in the output or response arises either due to the uncertainty associated with the governing system properties or due to the uncertainty in the input/source conditions. The input/source conditions are often spatially and/or temporally varying random processes in a natural hydrologic system. In the groundwater literature, the flow in the porous media was analyzed considering recharge as a spatial/temporal random input (Hantush and Marino 1994; Li and Graham 1999). Similarly in water quality modeling, a random biochemical oxygen demand (BOD) input to a stream, temperature, discharge, dissolved oxygen, decay etc. were analyzed in literature (Melching and Yoon 1996; Subbarao et al. 2004). Recently Wang and Zheng (2005) analyzed the contaminant transport under random sources in a groundwater system while assuming that the system parameters such as velocity of flow, porosity are deterministic. In their model, the random source was considered either as a continuous source with random fluctuations in time or as a discrete instantaneous source.

Stochastic modeling of flow and transport in a hydrologic system is necessitated when the parameters governing the system are treated as random fields. In the last three decades, several studies have been made for analyzing probabilistic behavior of flow and transport in the groundwater system considering parameters such as hydraulic conductivity, porosity, sorption coefficient etc as random fields. The results of such probabilistic analysis in solute transport studies were mainly presented either in terms of effective properties which were derived from spatial or temporal plume moments (Dagan 1989; Gelhar 1993; Hu et al. 1997; Huang and Hu 2000; Hassan 2001; Chaudhuri and Sekhar 2005a) or mean and standard deviation of concentration (Tang and Pinder 1979; Dagan 1989; Kapoor and Gelhar 1994).

The governing stochastic partial differential equations (SPDE) arising due to the presence of random

system parameters or random input conditions are often solved using either analytical or numerical approaches (de Marsily 1986). When analytical methods (Cushman 1997) are not applicable due to the complicated initial and source conditions, then non-uniform flow fields and non-stationary properties, numerical methods are often used. The popular and simple Monte Carlo simulation method (MCSM) is based on generating a large number of equally likely random realizations for obtaining statistical moments of the dependent variable while using a numerical method (e.g. finite difference, finite element, finite volume) for solution of the deterministic system for each realization (Bellin et al. 1992; Bosma et al. 1995; Hassan et al. 1999). This method is computationally exhaustive when a few thousands of realizations are required especially for a higher degree of medium heterogeneities along with higher space-time grid resolution. To avoid this difficulty associated with simulations involving multiple realizations, alternate methods such as perturbation based stochastic finite element method (SFEM) (Spanos and Ghanem 1989) were proposed. The SFEM was found to be a computationally attractive method for solving SPDEs. Recently, SFEM was applied in the groundwater literature for studying flow and transport of solutes in 3-D heterogeneous porous medium considering system parameters as random fields (Osnes and Langtangen 1998; Chaudhuri and Sekhar 2005b) and it was demonstrated that the method was computationally efficient in comparison with MCSM and was also accurate.

Studies dealing with SPDE's combining random description for source/boundary conditions along with system parameters are scarce. Li and Graham (1999) analyzed the effect of spatio-temporal random recharge on the contaminant transport problem in heterogeneous groundwater system. Using analytical methods, they found that the spreading of the mean concentration is enhanced when the random spatio-temporal variation of recharge is considered. In the engineering mechanics area the uncertainty in the input or loading is the main concern when the structure is subjected to random ground excitation due to earthquake or lateral wind loads. The system uncertainty arises from the random spatial distribution of Young's modulus and/or mass density. In such systems the probabilistic analysis of the response was performed using the SFEM coupled with theory of random vibration (Gao et al. 2004; Chaudhuri and Chakraborty 2006).

In the present study, a SFEM is proposed for solving flow and transport in a 3-D heterogeneous porous medium when both source conditions and system parameters are random. The source condition is assumed as a random discrete process while the system parameters viz. hydraulic conductivity, dispersivity, porosity, molecular diffusion coefficient, sorption coefficient and decay coefficient are treated as random fields. The probabilistic solution of concentration (i.e., mean and variance of concentration) for a deterministic unit pulse in such a stochastic system is obtained using SFEM. This solution is further used as a response function treating the source as a random process.

2 Problem definition

The governing equation for the transport of a linearly sorbing and decaying solute in a 3-D porous media is

$$\begin{aligned}&(n(\mathbf{x})+\rho_b k_d(\mathbf{x}))\frac{\partial c(\mathbf{x},t)}{\partial t}\\&+\frac{\partial}{\partial x_i}\left(n(\mathbf{x})v_i(\mathbf{x})c(\mathbf{x},t)-n(\mathbf{x})D_{ij}(\mathbf{x})\frac{\partial c(\mathbf{x},t)}{\partial x_j}\right)\\&+(n(\mathbf{x})+\rho_b k_d(\mathbf{x}))\gamma_d(\mathbf{x})c(\mathbf{x},t)=0,\end{aligned}\tag{1}$$

where $c(\mathbf{x},t)$ is the concentration at location $\mathbf{x}$ and time t. Here $n(\mathbf{x})$, $k_d(\mathbf{x})$ and γ_d $(\mathbf{x})$ are respectively spatially varying porosity, sorption and decay coefficient. In Eq. 1, $\mathbf{v}$ $(\mathbf{x})$ is the pore water velocity vector which is defined as $\mathbf{v}(\mathbf{x})=\mathbf{q}(\mathbf{x})/n(\mathbf{x})$. The seepage flux vector $\mathbf{q}$ $(\mathbf{x})$ is obtained using the hydraulic conductivity tensor $(\mathbf{K}(\mathbf{x}))$ and hydraulic head $(h(\mathbf{x}))$, based on the Darcy equation,

$$q_i(\mathbf{x})=-K_{ij}(\mathbf{x})\frac{\partial h(\mathbf{x})}{\partial x_j}.\tag{2}$$

It is to be noted that for the Eqs. 1 and 2, the Einstein convention of summation over double indices is implied unless otherwise specified. $\mathbf{D}(\mathbf{x})$ is the hydrodynamic dispersion coefficient tensor, which is combined with molecular diffusion coefficient (D_{m} $(\mathbf{x})$). The expression for it is given as

$$D_{ij}\mathbf{x}=\alpha(\mathbf{x})\left((1-\epsilon)\frac{v_i(\mathbf{x})v_j(\mathbf{x})}{v(\mathbf{x})}+\epsilon v(\mathbf{x})\delta_{ij}\right)+D_{\mathrm{m}}(\mathbf{x})\delta_{ij},\tag{3}$$

where $\alpha(\mathbf{x})$ is the longitudinal local dispersivity and ε is the ratio of transverse to longitudinal local dispersivity. The Eq. 1 is solved for a set of initial and boundary conditions, which in general, are written as

$$\begin{aligned}&c(\mathbf{x},0)=c_0(\mathbf{x}),\quad \text{for } \mathbf{x}\in\Omega,\\&c(\mathbf{x},t)=c_b(\mathbf{x},t),\quad \text{for } \mathbf{x}\in\Gamma_1,\\&\text{and}\\&\left(n(\mathbf{x})v_i(\mathbf{x})c(\mathbf{x},t)-n(\mathbf{x})D_{ij}(\mathbf{x})\frac{\partial c(\mathbf{x},t)}{\partial x_j}\right)n_{x_i}=f_b(\mathbf{x},t),\\&\qquad\text{for } \mathbf{x}\in\Gamma_2.\end{aligned}\tag{4}$$

Here $c_0(\mathbf{x})$ is initial distribution of concentration in the domain Ω while $c_b(\mathbf{x},t)$ and f_b $(\mathbf{x},t)$ are respectively the time-dependent specified concentration at the boundary Γ_1 and flux at the at the boundary Γ_2. Further n_{x_i} is the direction cosine of the normal to the boundary surface along x_i axis.

The equation for a steady state flow in the domain with spatially varying hydraulic conductivity field is given by

$$\frac{\partial}{\partial x_i}\left(K_{ij}(\mathbf{x})\frac{\partial h(\mathbf{x})}{\partial x_j}\right)=0, \tag{5}$$

with specified boundary conditions governing the flow in the domain represented as

$$h(\mathbf{x})=h_b(\mathbf{x}), \quad \text{for } \mathbf{x}\in\Gamma_1^h,$$

and

$$K_{ij}(\mathbf{x})\frac{\partial h(\mathbf{x})}{\partial x_j}n_{x_i}=q_b(\mathbf{x}), \quad \text{for } \mathbf{x}\in\Gamma_2^h. \tag{6}$$

3 Deterministic FEM formulation

In FEM the concentration inside an element is expressed as $c(\mathbf{x}, t)=\sum_{k=1}^{n} N_k(\mathbf{x})\, c_k(t)$, where n is the number of nodes per element. $N_k(\mathbf{x})$ and $c_k(t)$ are, respectively, kth shape function and concentration at kth node. For pth element the equation is obtained as

$$\begin{aligned}&\int_{\Omega^e}\left(n_p+\rho_b k_{d_p}\right)N_k(\mathbf{x})N_l(\mathbf{x})\mathrm{d}\mathbf{x}\frac{\mathrm{d}c_l(t)}{\mathrm{d}t}\\&\quad+\int_{\Omega^e}\left(\frac{\partial N_k(\mathbf{x})}{\partial x_i}\left(-n_p v_{i_p}N_l(\mathbf{x})+n_p D_{ij_p}\frac{\partial N_l(\mathbf{x})}{\partial x_j}\right)\right.\\&\quad\left.+(n_p+\rho_b k_{d_p})\gamma_{d_p}N_k(\mathbf{x})N_l(\mathbf{x})\right)\mathrm{d}\mathbf{x}c_l(t)\\&\quad+\oint_{\Gamma^e}N_k(\mathbf{x})\left(n_p v_{i_p}N_l(\mathbf{x})-n_p D_{ij_p}\frac{\partial N_l(\mathbf{x})}{\partial x_j}\right)\\&\quad\times n_{x_i}\mathrm{d}Sc_l(t)=0, \qquad (7)\\&\Rightarrow [R]_p\{\dot{c}(t)\}_p+[D]_p\{c(t)\}_p=\{c_b(t)\}_p. \qquad (8)\end{aligned}$$

Here the suffix 'p' corresponds to the property as well as the local matrix of pth element. The domain is discretized with N elements. The global equation for transport is obtained as

$$[R]\{\dot{c}(t)\}+[D]\{c(t)\}=\{c_b(t)\}. \tag{9}$$

Using the Crank–Nicholson formulation for the first-order time derivative, the global FE Eq. 9 can be further simplified as

$$\begin{aligned}&\frac{1}{\Delta t}[R]\{c^{t+1}-c^t\}+[D]\{\theta c^{t+1}+(1-\theta)c^t\}\\&\quad=\{\theta c_b^{t+1}+(1-\theta)c_b^t\}. \qquad (10)\end{aligned}$$

In the present study θ is taken as 0.5 to get a second-order accurate solution in time. Rearranging the terms, the equation for unknown concentration at the next time step in terms of the known concentration at previous time step and the boundary conditions, is written as

$$[D_1]\{c^{t+1}\}=[D_2]\{c^t\}+\theta\{c_b^{t+1}\}+(1-\theta)\{c_b^t\}, \tag{11}$$

where $[D_1]=\frac{1}{\Delta t}[R]+\theta[D]$ and $[D_2]=\frac{1}{\Delta t}[R]-(1-\theta)[D]$. These global transport matrices $[D_1]$ and $[D_2]$ as well as the source vectors $\{c_b^t\}$ and $\{c_b^{t+1}\}$ are formed by the given boundary conditions. Similar to the transport, the global equation for the flow for a given head and flux boundary conditions is obtained as

$$[K]\{h\}=\{h_0\}. \tag{12}$$

Here $[K]$ is the global hydraulic conductivity matrix in the flow equation. The ith component of seepage flux for pth element is obtained by taking average of that at all the Gauss points ($\mathbf{x}_k$, for $k=1,\ldots, N_G$, where N_G is the number of Gauss points) and is given as

$$\begin{aligned}q_{i_p}&=-\frac{1}{N_G}K_{ij_p}\sum_{k=1}^{N_G}\left.\frac{\partial N_l(\mathbf{x})}{\partial x_j}\right|_{\mathbf{x}_k}\\h_l&=-\frac{1}{N_G}K_p\sum_{k=1}^{N_G}\left.\frac{\partial N_l(\mathbf{x})}{\partial x_i}\right|_{\mathbf{x}_k}h_l.\end{aligned} \tag{13}$$

For isotropic cases the hydraulic conductivity tensor becomes a scalar quantity (K_p).

4 SFEM formulation

In a perturbation based SFEM, for each element, the properties which are treated as random variables are decomposed as $K_p=\bar{K}_p+K_p'$, $\alpha_p=\bar{\alpha}_p+\alpha_p'$, $n_p=\bar{n}_p+n_p'$, $k_{d_p}=\bar{k}_{d_p}+k_{d_p}'$, $\gamma_{d_p}=\bar{\gamma}_{d_p}+\gamma_{d_p}'$ and $D_{m_p}=\bar{D}_{m_p}+D_{m_p}'$. The pore water velocity and dispersion coefficient can also be written as $v_{i_p}=\bar{v}_{i_p}+v_{i_p}'$ and $D_{ij_p}=\bar{D}_{ij_p}+D_{ij_p}'$ respectively. For statistically homogeneous random field, the mean of the properties for each element remains the same. Hence the matrices ($[D_1]$, $[D_2]$, and $[K]$) are also decomposed into mean ($[\bar{D}_1]$, $[\bar{D}_2]$, and $[\bar{K}]$) and zero mean random perturbed components ($[D_1]'$, $[D_2]'$ and $[K]'$). The mean of the matrices are calculated at the expected value of the individual random parameters as well as their product given in Eq. 7. Under the approximation that the difference of the product of any two random variables and its ensemble average is negligible, the zero mean random perturbed part of transport matrices ($[D_1]'$ and $[D_2]'$) become linear functions of random variables r_p'. Here the random components (r_p', $p=1,2,\ldots, N_r$) correspond to the velocity, local dispersivity, molecular diffusion, porosity, sorption coefficient and decay coefficient of each element. N_r is the total number of random variables. The matrices $[D_1]$ and $[D_2]$ are expanded using the Taylor series about the mean value of the random properties (r_p', $p=1,2,\ldots, N_r$). Since the second and higher order derivatives of these matrices vanish being a linear case, the equations for the matrices can be given as

$$[D_1]=[\bar{D}_1]+[D_1]'=[\bar{D}_1]+\sum_{p=1}^{N_r}[D_1]_{r_p}^{(I)}r_p'$$

and

$$[D_2]=[\bar{D}_2]+[D_2]'=[\bar{D}_2]+\sum_{p=1}^{N_r}[D_2]_{r_p}^{(I)}r_p', \tag{14}$$

where $[D_1]^{(I)}_{r_p} = \frac{\partial [D_1]}{\partial r_p}$ and $[D_2]^{(I)}_{r_p} = \frac{\partial [D_2]}{\partial r_p}$. Similarly the concentration can be expanded in Taylor series about the value at mean of the random parameters and can be expanded as follows:

$$\{c^{t+1}\} = \{c^{t+1}\}^{(0)} + \sum_{p=1}^{N_r} \{c^{t+1}\}^{(I)}_{r_p} r'_p + \frac{1}{2}\sum_{p=1}^{N_r}\sum_{q=1}^{N_r} \{c^{t+1}\}^{(II)}_{r_p r_q} r'_p r'_q \cdots . \tag{15}$$

After substituting Eqs. 15 and 14 into Eq. 11, the various order of derivatives of concentration are obtained as

$$\{c^{t+1}\}^{(0)} = [\bar{D}_1]^{-1}\Big([\bar{D}_2]\{c^t\}^{(0)} + \theta\{c_b^{t+1}\} + (1-\theta)\{c_b^t\}\Big), \tag{16}$$

$$\{c^{t+1}\}^{(\mathrm{I})}_{r_p} = [\bar{D}_1]^{-1}\Big(-[D_1]^{(\mathrm{I})}_{r_p}\{c^{t+1}\}^0 + [D_2]^{(\mathrm{I})}_{r_p}\{c^t\}^0 + [\bar{D}_2]\{c^t\}^{(\mathrm{I})}_{r_p}\Big), \tag{17}$$

$$\{c^{t+1}\}^{(II)}_{r_p r_q} = [\bar{D}_1]^{-1}\Big(-[D_1]^{(\mathrm{I})}_{r_p}\{c^{t+1}\}^{(\mathrm{I})}_{r_q} - [D_1]^{(\mathrm{I})}_{r_q}\{c^{t+1}\}^{(\mathrm{I})}_{r_p} + [D_2]^{(\mathrm{I})}_{r_p}\{c^t\}^{(\mathrm{I})}_{r_q} + [D_2]^{(\mathrm{I})}_{r_q}\{c^t\}^{(\mathrm{I})}_{r_p} + [\bar{D}_2]\{c^t\}^{(\mathrm{II})}_{r_p r_q}\Big). \tag{18}$$

It is noted that $[D_1]^{(\mathrm{I})}_{q,r_p}$ and $[D_2]^{(\mathrm{I})}_{q,r_p}$ do not vanish when r_p corresponds to any property of qth element. Hence, the derivative of global matrices $[D_1]^{(\mathrm{I})}_{r_p}$ and $[D_2]^{(\mathrm{I})}_{r_p}$ have nonzero entry in the position corresponding to qth element and the collection of all nonzero entries in $[D_1]^{(\mathrm{I})}_{r_p}$ and $[D_2]^{(\mathrm{I})}_{r_p}$ forms a matrix of size same as $[D_1]_q$ and $[D_2]_q$ respectively. This procedure helps to reduce the computational time by several orders (Chaudhuri and Sekhar 2005b). It may be noted here that the perturbation based SFEM is intrinsically limited to moderately fluctuating random fields or better, to random fields with small variances as the perturbation expansion in the fluctuations of the random fields and subsequent averaging leads to expansion of quantities of interest in the variance of the random fields.

The covariance matrix of the random properties (which are piece-wise linear inside an element), are derived from the given variances and spatial correlation functions for the random fields. In the later section, a brief description of the random properties and the procedure to obtain the covariance matrix are provided. For solving the transport problem, the mean and covariance of velocity vectors and dispersion coefficient tensors are required to be derived, which are obtained from the mean and covariance of hydraulic conductivity and local scale dispersivity. The equations and the procedure for obtaining these stochastic quantities of velocity and dispersion coefficient are separately given in the Sect. 11.

5 Random source condition

The concentration of the source is assumed as a random process. A random source may be in the form of random timing, random location and random amount of mass loading (Wang and Zheng 2005). The random sources can be categorized into two types: those occurring continuously with a deterministic component and random variations and those occurring randomly at instantaneous, discrete-time instances. In this work, discrete type of source with random amount of mass injection is considered. The location and the timing of the source is assumed to be known. When the mass is released instantaneously at discrete-time points, the total amount of cumulative mass in the system is the sum of random number of incidents: $\sum_{k=1}^{M(t)} c_{A_k}$, where $M(t)$ is the number of mass releases that occurred during the interval [0, t]. In the present study, the mass releases are assumed to be at constant known time intervals. Here c_{A_k} is the amount of random mass released at time τ_k. It is also assumed in this study that the magnitude of the mass released at each time follows a normal distribution, however the formulation can consider any distribution.

Figure 1 illustrates a typical realization of random, discrete-time mass events. In the present work, for the solute transport problem under the general assumptions, the concentration at any location ($\mathbf{x}$) and time (t) can be obtained as a random sum of the impulse/response function, which is expressed as

$$c(\mathbf{x}, t) = \sum_{k=1}^{M(t)} c_{A_k} G_c(\mathbf{x}, t, \tau_k). \tag{19}$$

In the above expression, G_c ($\mathbf{x}$,t,τ_k) is a response function of the concentration in a 3-D porous medium, due to a unit magnitude of mass of solute, which is applied at the top of the domain at time $t = 0$ following a given set of boundary conditions. Since the response function must satisfy the condition: G_c ($\mathbf{x}$,t,τ) = 0 for $t < \tau$, in the Eq. 19, $M(t)$ can be replaced by $M(T)$ where T is the total time of simulation. Since the output concentration here is a nonlinear function of system parameters, hence a truncated Taylor series

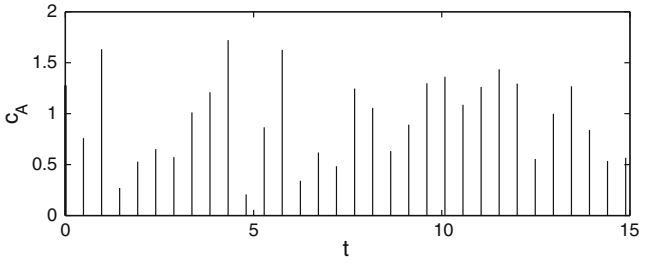

Fig. 1 A typical realization of random mass release at constant time interval

expansion is used for the stochastic analysis of output concentration while incorporating the uncertainty in the system parameters. When numerical methods are used for the solution with discretization in space and time, the response function is obtained as a vector of concentration at all nodes $\{G_c(t,\tau_k)\}$. The concentration at ith node due to the multiple sources can be expressed as,

$$c_i(t) = \sum_{k=1}^{M(T)} c_{A_k} G_{c_i}(t,\tau_k). \tag{20}$$

When the governing transport parameters are also random fields, the Eq. 20 can be further expressed as,21

$$c_i(t) = \sum_{k=1}^{M(T)} c_{A_k}\left((G_{c_i}(t,\tau_k))^{(0)} + \sum_{p=1}^{N_r} (G_{c_i}(t,\tau_k))^{(\mathrm{I})}_{r_p} r'_p + \frac{1}{2}\sum_{p=1}^{N_r}\sum_{q=1}^{N_r} (G_{c_i}(t,\tau_k))^{(\mathrm{II})}_{r_p r_q} r'_p r'_q \right). \tag{21}$$

The random transport parameters are usually uncorrelated with the source conditions i.e. c_{A_k} and r'_p are uncorrelated. Taking the expectation of the Eq. 21 the mean concentration is obtained as,22

$$\bar{c}_i(t) = \sum_{k=1}^{M(T)} \bar{c}_{A_k}\left((G_{c_i}(t,\tau_k))^{(0)} + \frac{1}{2}\sum_{p=1}^{N_r}\sum_{q=1}^{N_r} (G_{c_i}(t,\tau_k))^{(\mathrm{II})}_{r_p r_q} \overline{r'_p r'_q} \right) = \sum_{k=1}^{M(t)} \bar{c}_{A_k} \bar{G}_{c_i}(t,\tau_k). \tag{22}$$

To obtain the cross covariance of concentration the expression of the expectation of the product of concentration at two different times and nodes is written as,

$$\begin{aligned}\overline{c_i(t_1)c_j(t_2)} = \sum_{k=1}^{M(T)}\sum_{l=1}^{M(T)} \overline{c_{A_k}c_{A_l}}\Big(&(G_{c_i}(t_1,\tau_k))^{(0)} \times \left(G_{c_j}(t_2,\tau_l)\right)^{(0)} + \sum_{p=1}^{N_r}\sum_{q=1}^{N_r}\Big((G_{c_i}(t_1,\tau_k))^{(\mathrm{I})}_{r_p} \\ &\times \left(G_{c_j}(t_2,\tau_l)\right)^{(\mathrm{I})}_{r_q} + \frac{1}{2}\Big((G_{c_i}(t_1,\tau_k))^{(0)} \\ &\times \left(G_{c_j}(t_2,\tau_l)\right)^{(\mathrm{II})}_{r_p r_q} + (G_{c_i}(t_1,\tau_k))^{(\mathrm{II})}_{r_p r_q} \\ &\times \left(G_{c_j}(t_2,\tau_l)\right)^{(0)}\Big)\Big)\overline{r'_p r'_q}\Big).\end{aligned} \tag{23}$$

Here the expectation of the product of more than two random varibles are neglected. Since the random pulse input of concetration at two different times are indepandent, one can note that

$$\overline{c_{A_k}c_{A_l}} = (\bar{c}_A)^2 + \sigma^2_{c_A}\delta_{kl}. \tag{24}$$

The cross-covariance of concentration is obtained as

$$\begin{aligned}C_{c_i c_j}(t_1,t_2) &= \overline{c'_i(t_1)c'_j(t_2)} = \overline{c_i(t_1)c_j(t_2)} - \bar{c}_i(t_1)\bar{c}_j(t_2) \\ &= \sum_{k=1}^{M(T)} \sigma^2_{c_A}\Big((G_{c_i}(t_1,\tau_k))^{(0)}\left(G_{c_j}(t_2,\tau_k)\right)^{(0)} \\ &\quad + \sum_{p=1}^{N_r}\sum_{q=1}^{N_r}\Big((G_{c_i}(t_1,\tau_k))^{(\mathrm{I})}_{r_p}\left(G_{c_j}(t_2,\tau_k)\right)^{(\mathrm{I})}_{r_q} \\ &\quad + \frac{1}{2}\Big((G_{c_i}(t_1,\tau_k))^{(0)}\left(G_{c_j}(t_2,\tau_k)\right)^{(\mathrm{II})}_{r_p r_q} \\ &\quad + (G_{c_i}(t_1,\tau_k))^{(\mathrm{II})}_{r_p r_q}\left(G_{c_j}(t_2,\tau_k)\right)^{(0)}\Big)\overline{r'_p r'_q}\Big) \\ &\quad + \sum_{k=1}^{M(T)}\sum_{l=1}^{M(T)} (\bar{c}_A)^2 \sum_{p=1}^{N_r}\sum_{q=1}^{N_r} (G_{c_i}(t_1,\tau_k))^{(\mathrm{I})}_{r_p} \\ &\quad \times \left(G_{c_j}(t_2,\tau_l)\right)^{(\mathrm{I})}_{r_q}\overline{r'_p r'_q}.\end{aligned} \tag{25}$$

In deriving the random component of the concentration, the term $r'_p r'_q - \overline{r'_p r'_q}$ has been ignored, which results in the first-order accurate covariance matrix of concentration. The standard deviation of concentration, $\sigma_{c_i}(t) = \sqrt{\overline{c'_i(t)c'_i(t)}}$ increases due to additive effect of source uncertainty. If the unit response function at any location in the domain is obtained using SFEM for the specified unit pulse source condition, the mean and covariance of concentration for a random source condition at that location can be obtained using the Eqs. 22 and 25, respectively. These expressions of mean and covariance of concentration can also be applicable when the source is a random continuous process after discretizing the continuous source into a series of random multiple pulses. The covariance of source concentration at different times $\overline{c_{A_k}c_{A_l}}$ is obtained from the known mean and autocorrelation function of the random source condition.

6 Descriptions of the random fields

In this study all the flow and transport properties, which are considered as random fields, are assumed to follow a log normal distribution since they take positive values and also vary considerably. However this assumption is not a limitation for the proposed SFEM. For any spatially varying random field, the correlation coefficient between any two locations is described by a correlation function. In this study, the random fields are assumed as statistically homogeneous and described by a Gaussian (squared exponential) type correlation function, which is defined as, $\rho(\mathbf{x}) = \exp\left(-\left(\frac{x_1}{\lambda_1}\right)^2 - \left(\frac{x_2}{\lambda_2}\right)^2 - \left(\frac{x_3}{\lambda_3}\right)^2\right)$. Here ($x_1$, x_2, x_3) are the separation distance between two points in the Cartesian coordinate system, while λ_1, λ_2 and λ_3 are the correlation lengths, which describe the scale of variability in space. However, it may be noted that for specific applications experimentally derived

correlations functions, if available can also be used in the SFEM. The covariance matrix for the discretized field of the random parameters is determined from the above correlation function and the variances of the parameters using the local averaging method (Vanmarcke 1983). Using this method the correlation coefficient of logarithmic of parameters, f_p and f_q of pth and qth elements respectively, is obtained as,

$$\rho_{f_p f_q} = \frac{1}{V_p V_q} \int_{V_p} \int_{V_q} \rho(\mathbf{x}_p - \mathbf{x}_q) \mathrm{d}\mathbf{x}_p \mathrm{d}\mathbf{x}_q. \tag{26}$$

Further the correlation coefficient between any two random parameters can be determined from the correlation coefficient of the corresponding logarithmic parameters. For example the correlation coefficient between K_p and k_{d_q} can be obtained from the standard deviation of log parameters (σ_{f_K} and $\sigma_{f_{k_d}}$) and correlation coefficient $\rho_{f_{K_p} f_{k_{dq}}}$. This is given as,

$$\rho_{K_p k_{dq}} = \frac{K_G k_{d_G}}{\sigma_K \sigma_{k_d}} \exp\left(\frac{1}{2}\left(\sigma^2_{f_K} + \sigma^2_{f_{k_d}}\right)\right) \times \left(\exp\left(\rho_{f_{K_p} f_{k_{dq}}} \sigma_{f_K} \sigma_{f_{k_d}}\right) - 1\right). \tag{27}$$

7 Results and discussions

The methodology developed in the Sects. 4 and 5 combining SFEM with random source conditions is applied to the problem of solute transport in a 3-D heterogeneous medium with random contaminant source located at the top domain of the soil system as illustrated in the Fig. 2. The solute from this source at the top of the domain is assumed to get transported through the under lying soil layers by both vertical recharge and horizontal subsurface flow. The governing parameters for flow and transport are assumed to vary randomly in space.

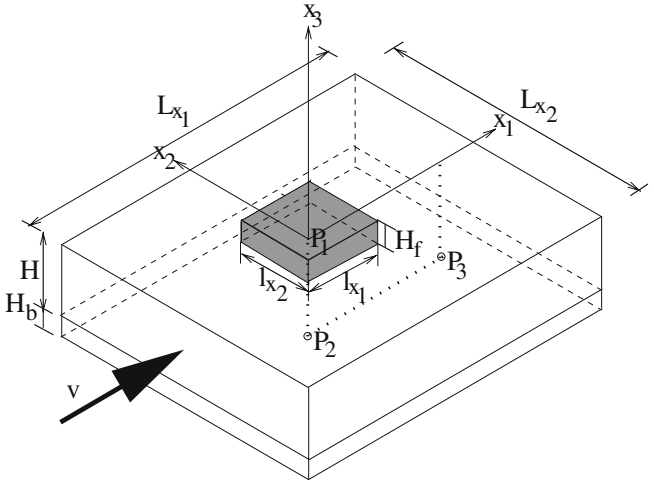

Fig. 2 Schematic diagram of 3-D domain with a source at the top surface of the soil layer

A typical mixed flux boundary condition is used here, which is based on the 1-D vertical transport of leachate from a source (Rowe and Booker 1986). It is assumed that the source has an initial specified mass of contaminant with a known concentration (c_0). The total mass of pollutant in the source decreases with time as it leaches down. Hence a time varying concentration boundary condition has to be applied at the source location. The top boundary condition for this problem may be given as,

$$c(\mathbf{x}, t) = c_0 - \frac{1}{H_f} \int_0^t f(\mathbf{x}, \tau) \mathrm{d}\tau \quad \text{for } -\frac{l_{x_1}}{2} \le x_1 \le \frac{l_{x_1}}{2}, -\frac{l_{x_2}}{2} \le x_2 \le \frac{l_{x_2}}{2} \text{ and } x_3 = 0. \tag{28}$$

This boundary condition can be rewritten as,

$$f(\mathbf{x}, t) = -H_f \frac{\partial c(\mathbf{x}, t)}{\partial t} \text{ and } c(\mathbf{x}, 0) = c_0 \quad \text{for } -\frac{l_{x_1}}{2} \le x_1 \le \frac{l_{x_1}}{2}, -\frac{l_{x_2}}{2} \le x_2 \le \frac{l_{x_2}}{2} \text{ and } x_3 = 0, \tag{29}$$

where the solute flux is expressed as, $f(\mathbf{x}, \tau) = \left(n(\mathbf{x}) v_i(\mathbf{x}) c(\mathbf{x}, t) - n(\mathbf{x}) D_{ij}(\mathbf{x}) \frac{\partial c(\mathbf{x}, t)}{\partial x_j}\right) n_{x_i}$. At the top surface $n_{x_1} = 0$ and $n_{x_2} = 0$. In the Eq. 29 H_f is the height of the leachate source. It is considered that soil is stratified below the source with upper layer close to the source having a lower permeability while the bottom layer having a higher permeability. In this study the correlation scales along the horizontal plane is assumed to be same (i.e. $\lambda_1 = \lambda_2 = \lambda_h$). The horizontal correlation scale (λ_h) is considered much larger in comparison to the vertical correlation scale (λ_v). The flow-field in this problem becomes non-uniform due to the constant continuous recharge from the pollutant source combined with lateral groundwater flow in the permeable layer.

The mean and covariance of the random flow field is derived from the random hydraulic conductivity field. Along with covariance matrices of the other random fields, the covariance of velocity is also used for the probabilistic analysis of contaminant transport. A square contaminant source of dimension $l_{x_1} = l_{x_2} = l$ is assumed to be located in an aquifer. The governing Eq. 1, the boundary conditions in Sect. 2 and the parameters are made dimensionless with respect to the size of the source and the horizontal velocity of flow. Here $c(\mathbf{x}, t) = \tilde{c}(\tilde{\mathbf{x}}, \tilde{t})/c_0$ is the dimensionless concentration of the pollutant at a dimensionless distance $\mathbf{x} = \tilde{\mathbf{x}}/l$, a dimensionless time ($t = v_d \tilde{t}/l$) and c_0 is the concentration at the top of the soil. Further, $\mathbf{v}(\mathbf{x}) = \tilde{\mathbf{v}}(\tilde{\mathbf{x}})/v_d$, $\alpha(\mathbf{x}) = \tilde{\alpha}(\tilde{\mathbf{x}})/l$, $D_m(\mathbf{x}) = \tilde{D}_m(\tilde{\mathbf{x}})/(v_d l)$, $\gamma_d(\mathbf{x}) = \tilde{\gamma}_d(\tilde{\mathbf{x}}) l/v_d$ and $q = \tilde{q}/v_d$ are respectively the dimensionless velocity of flow, dispersivity, molecular diffusion, decay coefficient and recharge at the top. Here v_d is the horizontal

velocity of flow, for a deterministic case without any recharge. The following numerical values of parameters are chosen for solving the 3-D problem: $\bar{n} = 0.4$, $\rho_b \bar{k}_d = 0.5$, $\bar{\gamma}_d = 0.4$, $\bar{\alpha} = 0.2$, $\bar{D}_m = 0.2$, $q = 0.5$, $\varepsilon = 0.1$. The dimensionless correlation lengths with respect to the size of the source are: $\lambda_h = 2.0$ and $\lambda_v = 0.5$. The dimensionless thickness of low permeable upper layer, $l_{x_3} = 0.5$ and high permeable low layer, $H_b = 0.01$. The coefficient of variation (COV) of the random parameters are provided in the Table 1.

7.1 Analysis for a unit pulse

The mean and standard deviation of the concentration at various locations in the domain for a unit deterministic concentration pulse condition at the source is computed using SFEM. It may be noted that these mean and standard deviations are a function of the random hydraulic conductivity, porosity, dispersivity, molecular diffusion coefficient, sorption coefficient and decay coefficient. Figures 3, 4, 5, 6, 7 show the temporal variation of the mean and standard deviations for various cases (listed in Table 1) at locations: P_1 (0, 0, 0), P_2 (0, 0, −0.5), P_3 (2.5, 0, −0.5), P_4 (−1.0, 0, −0.5), and P_5 (0, −1.0, −0.5). These locations P_1–P_5 are shown in Fig. 2. At the bottom of the source (location, P_1), the mean concentration is found to have a maximum value initially, which decreases exponentially with time while the standard deviation of concentration is initially zero and attains a peak value after a time lag. This behavior is expected for a deterministic initial source condition. At P_2–P_5, which are located at the bottom of the permeable layer (away from the source), both the mean and the standard deviation of concentration are initially zero. The mean concentration exhibits a peak after some time lag and the peak is delayed and its magnitude decreases with an increase in the distance of the location from the source. Interestingly, it is observed that the standard deviation of concentration shows two peaks when mean concentration changes rapidly, since it is calculated from the derivative of the concentration.

The results of mean and standard deviation in the above locations are compared for various cases (Cases A–F). Cases B–F correspond to the cases with system parameters being random while Case A deals with a deterministic system. The Cases B–F differ from each other depending on the magnitudes of coefficient of variation of system parameters, height of the source condition (H_f) and the ratio of permeabilities of stratified layers below the source (R_K). The diffusion coefficient of bottom layer is assumed to be (R_K/5) times of that of upper layer. The mean concentration at P_2 and

Table 1 The parameters used for various Cases A–F

Case	H_f	R_K	COV_K	COV_η	COV_{k_d}	COV_{γ_d}	COV_α	COV_{D_m}
A	0.2	100	0.0	0.0	0.0	0.0	0.0	0.0
B	0.2	100	0.4	0.4	0.4	0.4	0.4	0.4
C	0.2	100	1.0	0.4	0.4	0.4	0.4	0.4
D	0.1	100	1.0	0.4	0.4	0.4	0.4	0.4
E	0.2	50	1.0	0.4	0.4	0.4	0.4	0.4
F	0.1	50	1.0	0.4	0.4	0.4	0.4	0.4

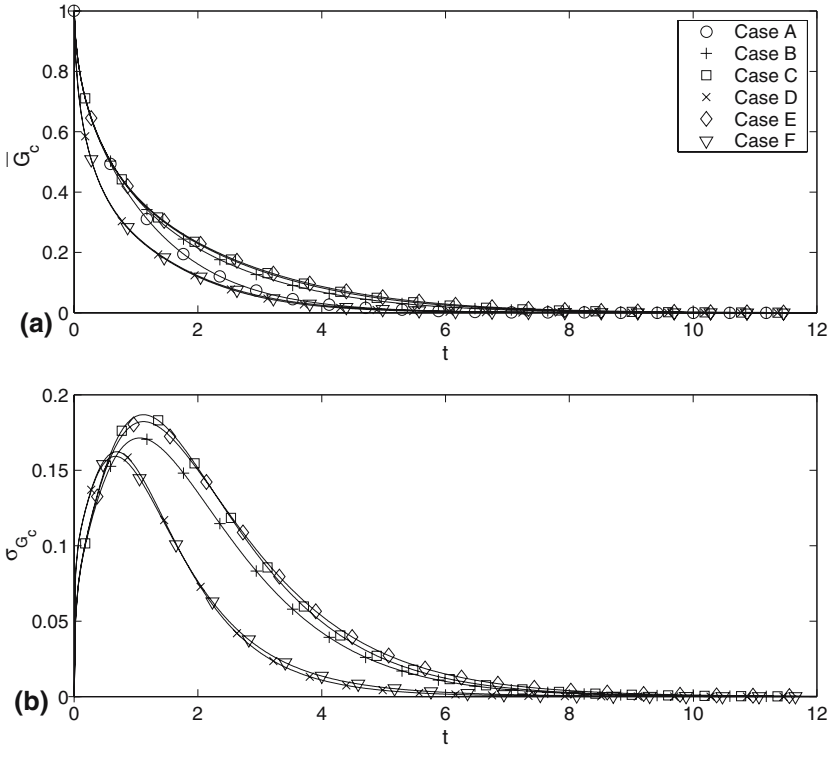

Fig. 3 The temporal variation of concentration at location P_1 for various cases due to a unit concentration pulse as a source condition

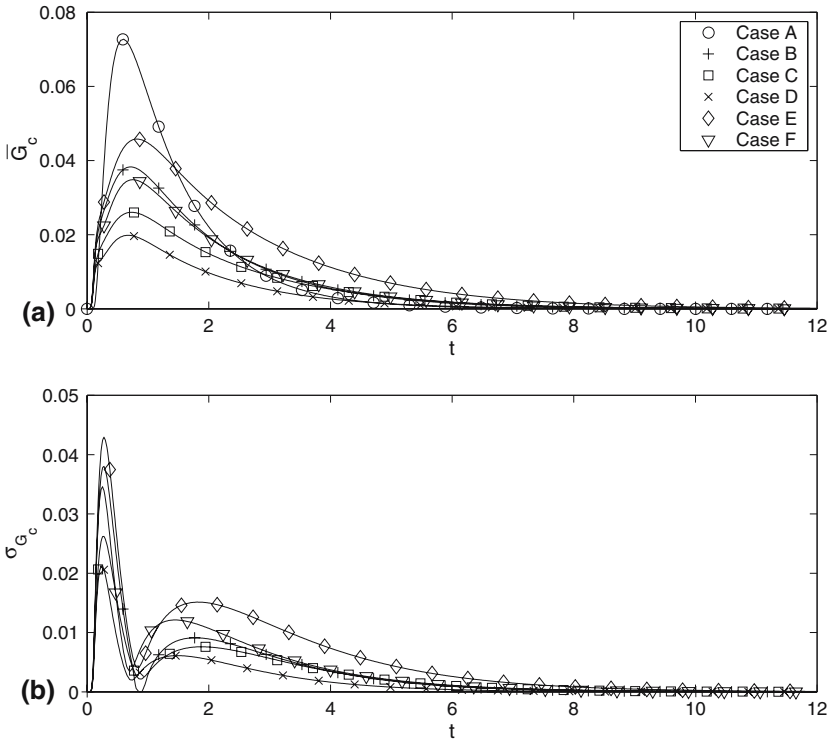

Fig. 4 The temporal variation of concentration at location P_2 for various cases due to a unit concentration pulse as a source condition

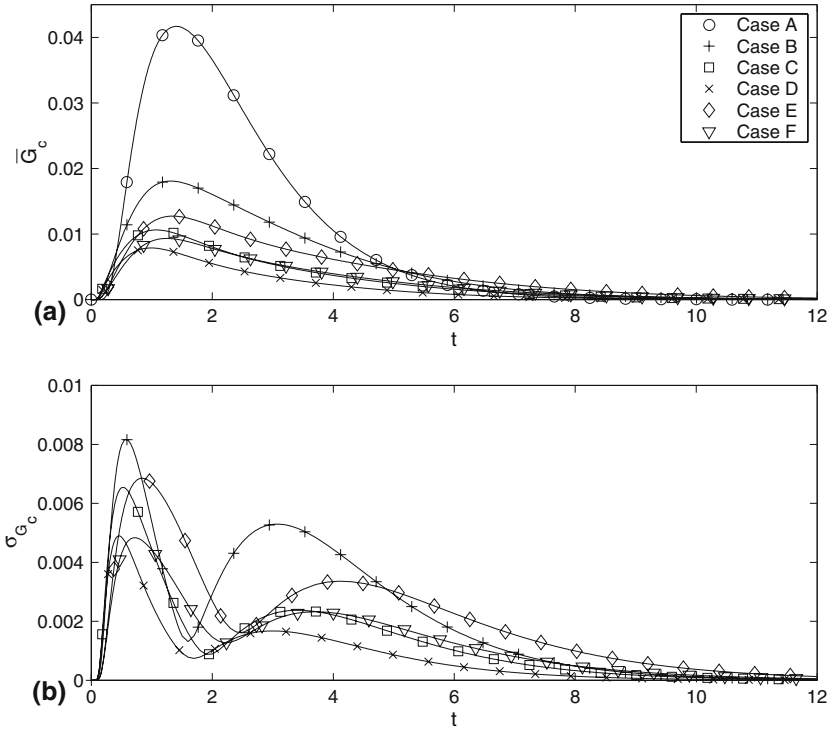

Fig. 5 The temporal variation of concentration at location P_3 for various cases due to a unit concentration pulse as a source condition

P_3 (along the flow direction), is observed to decrease with increasing coefficient of variation (Cases A, B and C). In contrary, the mean concentration for Case A (deterministic system) is always lesser than stochastic system at locations P_4 (upstream of the source) and P_5 (transverse to the flow path). This contrasting behavior of mean concentration around the source is due to the fact that the uncertainty in the hydraulic conductivity field reduces the effective velocity while enhancing the spreading of solutes. In most of the locations the mean concentration for Case B is lying in between Cases A and C. In general as the uncertainty in the hydraulic conductivity is increased, the mean concentration downstream of the source in the longitudinal direction

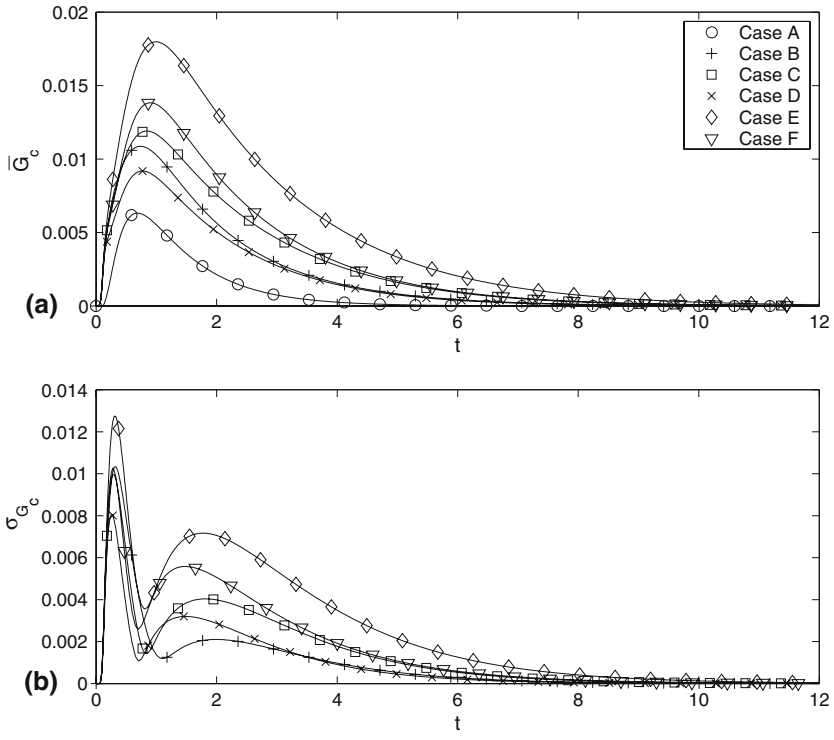

Fig. 6 The temporal variation of concentration at location P_4 for various cases due to a unit concentration pulse as a source condition

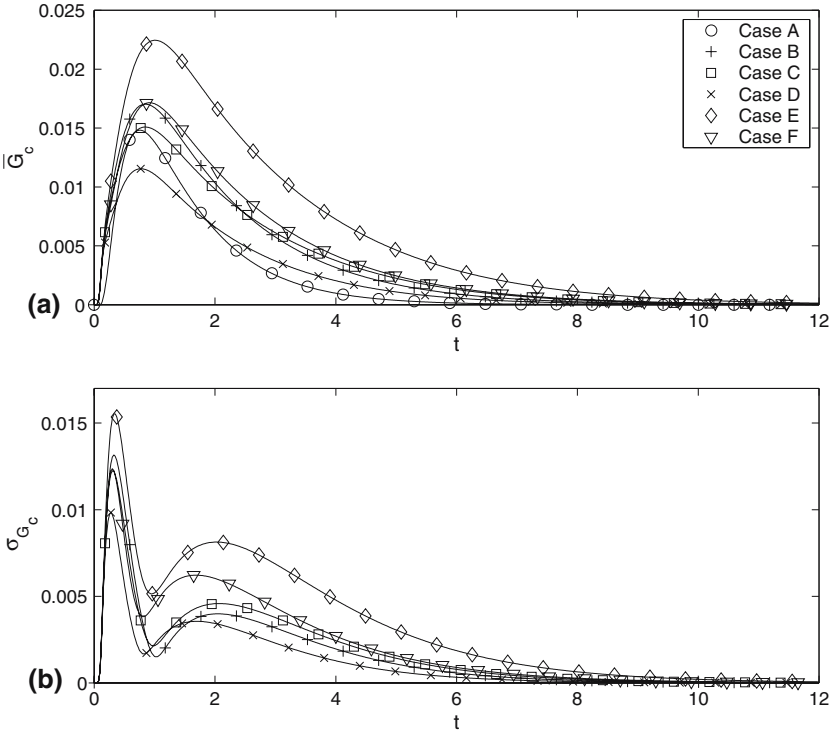

Fig. 7 The temporal variation of concentration at location P_5 for various cases due to a unit concentration pulse as a source condition

decreases. However, a contrasting behavior is observed at the upstream of source. As the solute is moving slower for Case C and in the presence of decay parameter, results in a lower mean concentration along the downstream direction. The standard deviation of concentration has a similar behavior as the mean concentration at P_1–P_5 when comparing between Cases B and C. It is interesting to note that the standard deviation of concentration is lower at downstream locations P_2 and P_3 for Case C (a case with higher uncertainty in hydraulic conductivity) essentially due to a lower mean concentration at these locations.

Further, the mean and standard deviation of concentration are compared for Cases C–F. Since the amount of solute mass input is twice in Case C in comparison to Case D, the mean and standard deviation of concentration at all locations are higher when the height of the source (H_f) is larger. However, it is observed that the effect of H_f is not linear and not same at all locations. This effect is found to be marginally higher at locations close to the source. The amount of solute mass input is twice in Case C in comparison to Case D.

When the hydraulic conductivity and diffusion coefficient of the lower layer are higher (comparison of Cases C and E or D and F), the mean and standard deviation of concentration at locations P_2–P_5 (at the bottom of low conductive layer) are found to be higher. Since the spreading of concentration is quicker and higher due to higher hydraulic conductivity and/or diffusion coefficient, the mean concentration in such a case close to the source exhibits a lower concentration. Accordingly the standard deviation of concentration is also lower. However, at the tail ends of the plume, the mean concentration can be higher, which may result in contrasting signature to the one observed above. Further, the results at location P_1 are not much influenced by R_K as this is at the source location and dispersion effects are minimal.

The auto-covariance of concentration at locations (P_2–P_5) as presented in Fig. 8 are not always positive. This behavior of auto-covariance function corresponds to the bimodal temporal behavior of standard deviation of concentration. In contrast as standard deviation behavior is unimodal in time at P_1, correspondingly the auto-covariance exhibits a positive surface. The auto-covariance of concentration is used to compute the last term in the Eq. 25 during calculation of the auto-covariance of concentration for multiple random pulses.

7.2 Analysis for multiple random pulses

In this section, analysis is extended for assessing the probabilistic behavior of concentration distribution in

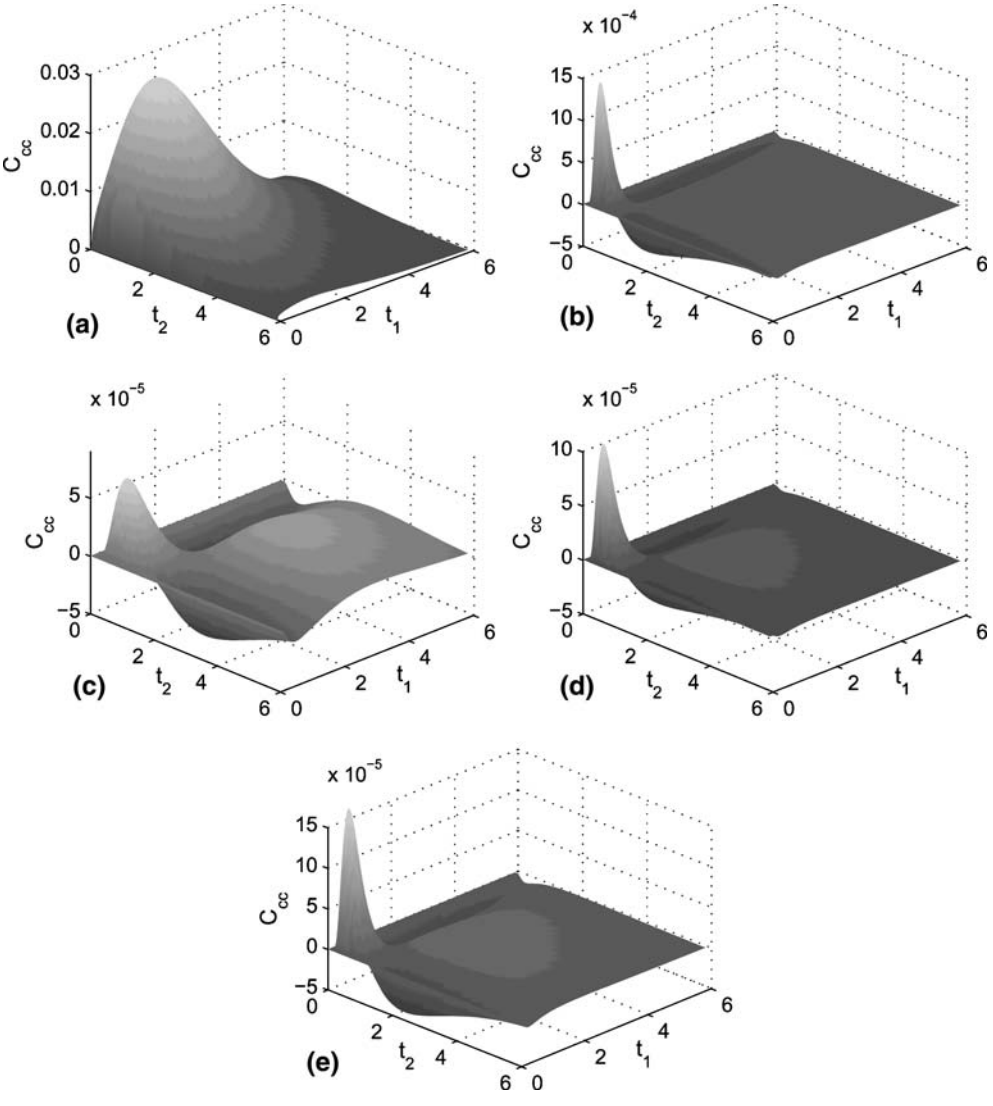

Fig. 8 The covariance of concentration with time at various locations: **a** P_1, **b** P_2, **c** P_3, **d** P_4 and **e** P_5

the domain (Fig. 2) due to a multiple random source pulses. Here it is assumed that the randomness in the pulses correspond to their magnitude while keeping a specified constant time interval among them. The response function obtained in the previous section for a single unit deterministic pulse is used with the procedure described in the Sect. 5 for multiple random pulses to obtain the mean and standard deviation of concentration at various locations. Figures 9, 10, 11, 12, 13 present a typical realization of the concentration breakthrough curve due to the random source condition as shown in Fig. 1 in addition to the temporal behavior of the mean and standard deviation of concentration at locations P_1–P_5 respectively. Comparison between the Cases A and B is made in Figs. 9, 10, 11, 12, 13 which correspond to either a deterministic or stochastic system in the presence of random multiple source condition. The mean and standard deviation of concentration behavior shows a pattern of reaching a steady-state condition, which is expected due to multiple pulses. Due to the assumption of constant interval between the pulses, the mean and standard deviation shows a fluctuating response with the same frequency. If the frequency of the pulses is very high (interval between the pulses is very low) then the fluctuating pattern in them may not be distinguishable. Since the response function of concentration at far away location is wider and relatively more flat, it is observed in Figs. 9, 10, 11, 12, 13 that the concentration break through curve becomes smoother at large time as the distance from the source increases.

As expected it is observed that mean and standard deviation of concentration are affected by the uncertainty in the system parameters. However, the uncertainty in the source condition is not affecting the mean concentration (as shown in Figs. 9b, 10b, 11b, 12b, 13b). This may be expected from the nature of the equation for the mean (Eq. 22). The behavior of mean concentration for single deterministic pulse as well as multiple random pulses is very similar when compared between deterministic and stochastic system (Cases A and B). The standard deviation of concentration is affected by both the uncertainty in the system parameters and the source condition. The standard deviation of concentration (as shown in Figs. 9c, 10c, 11c, 12c, 13c) is found to be higher when the source condition is treated as random process than the case of deterministic source condition. The time averaged mean and coefficient of variation at large time are compared between the uncertainty in source condition and system parameters for various Cases A–F and are listed in the Table 2. From the results of various cases at different locations it is observed that the coefficient of variation increases approximately by 25% due to the uncertainty in the source condition when both the system parameters and source condition have same level of uncertainty. At location P_1, the effect of uncertainty in the source condition is marginally

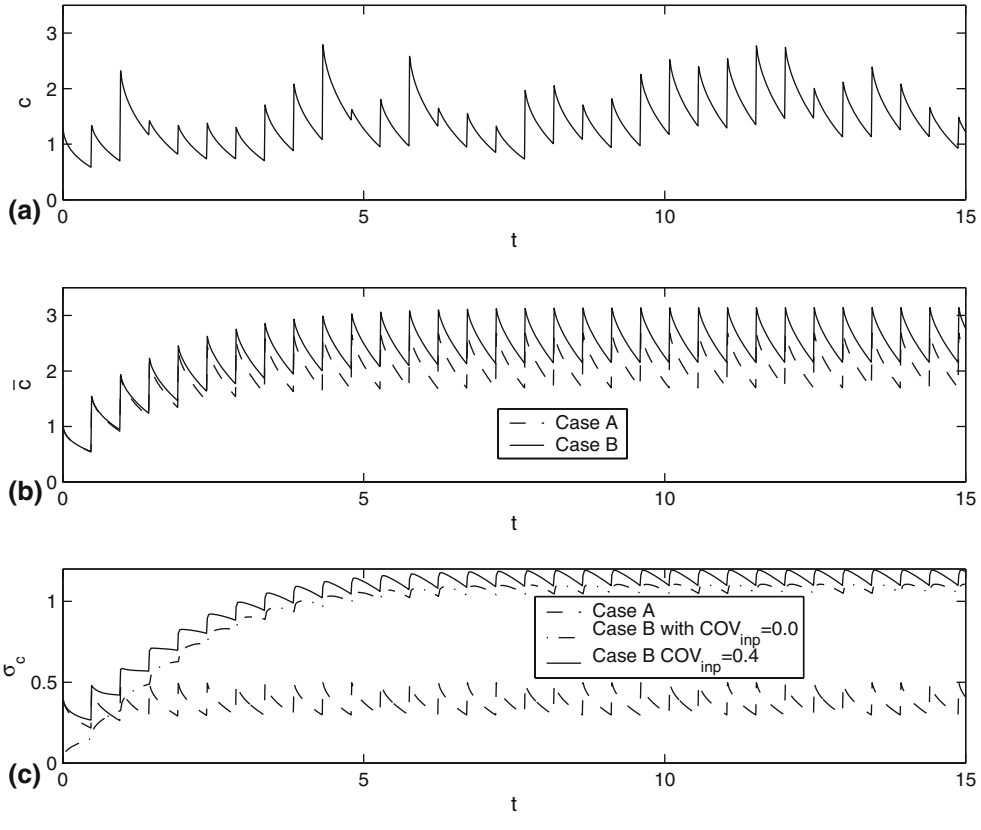

Fig. 9 The temporal behavior of concentration at location P_1 due to multiple random source pulses. **a** Break through curve of a single realization. **b** Comparison of mean concentration between Cases A and B. **c** Comparison of standard deviation of concentration between Cases A and B with deterministic source ($COV_{inp} = 0.0$) and random source ($COV_{inp} = 0.4$)

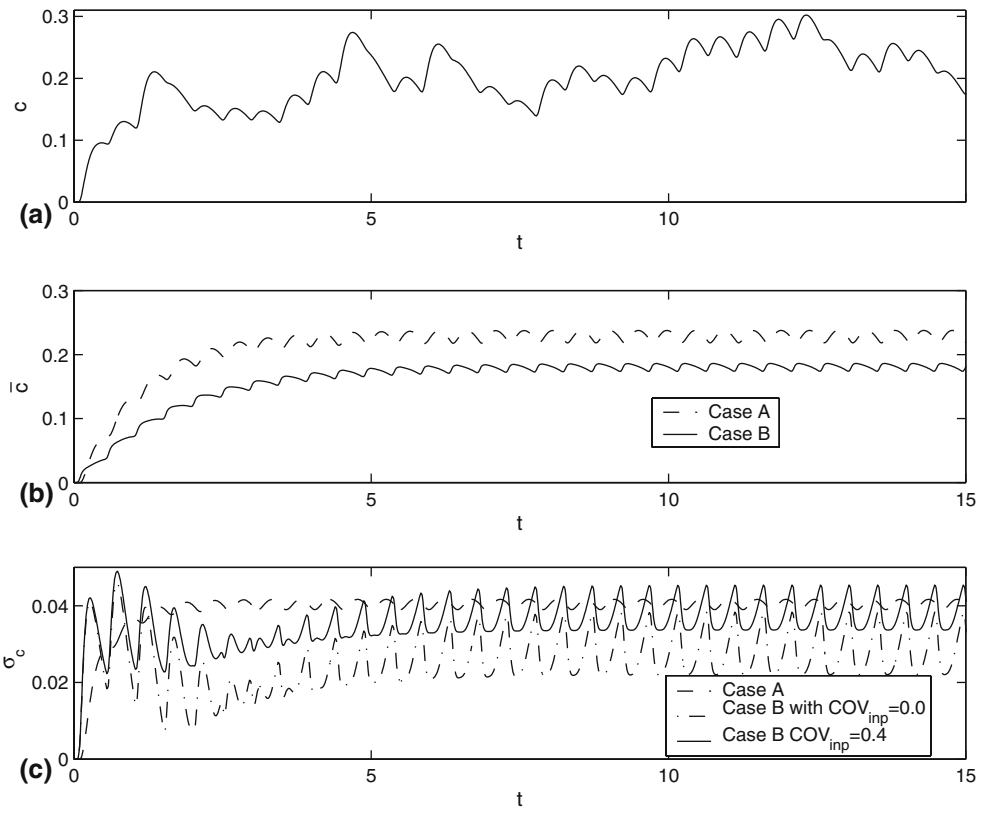

Fig. 10 The temporal behavior of concentration at location P_2 due to multiple random source pulses. **a** Break through curve of a single realization. **b** Comparison of mean concentration between Cases A and B. **c** Comparison of standard deviation of concentration between Cases A and B with deterministic source ($COV_{inp} = 0.0$) and random source ($COV_{inp} = 0.4$)

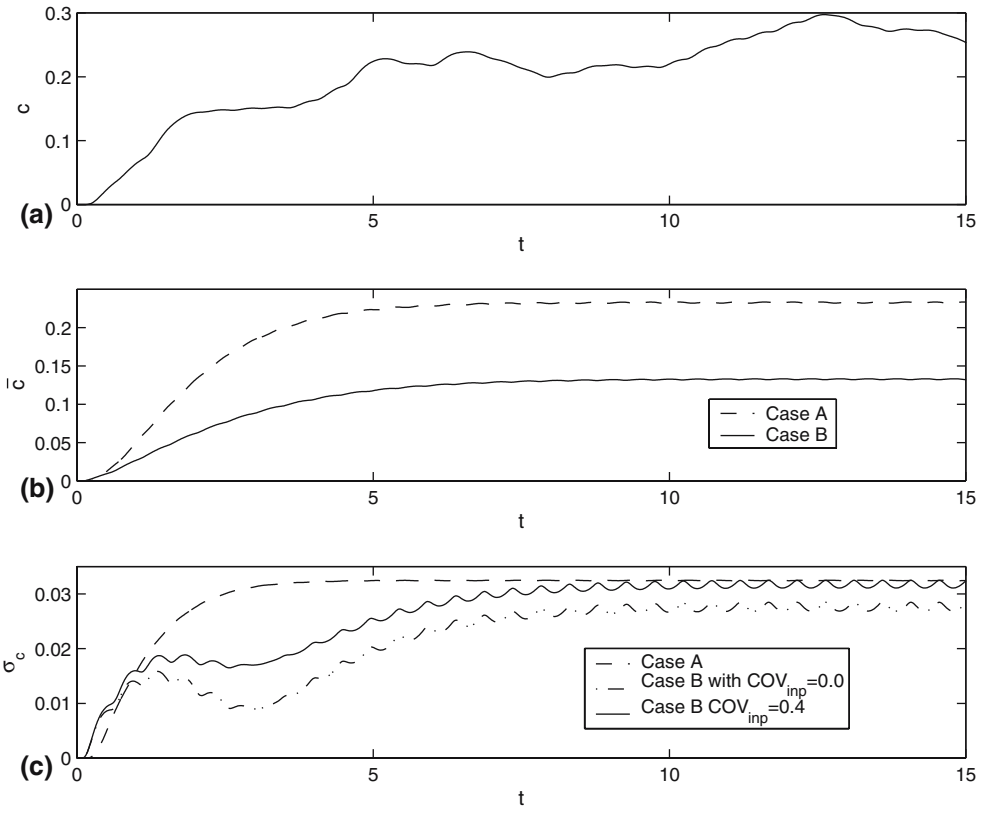

Fig. 11 The temporal behavior of concentration at location P_3 due to multiple random source pulses. **a** Break through curve of a single realization. **b** Comparison of mean concentration between Cases A and B. **c** Comparison of standard deviation of concentration between Cases A and B with deterministic source ($COV_{inp} = 0.0$) and random source ($COV_{inp} = 0.4$)

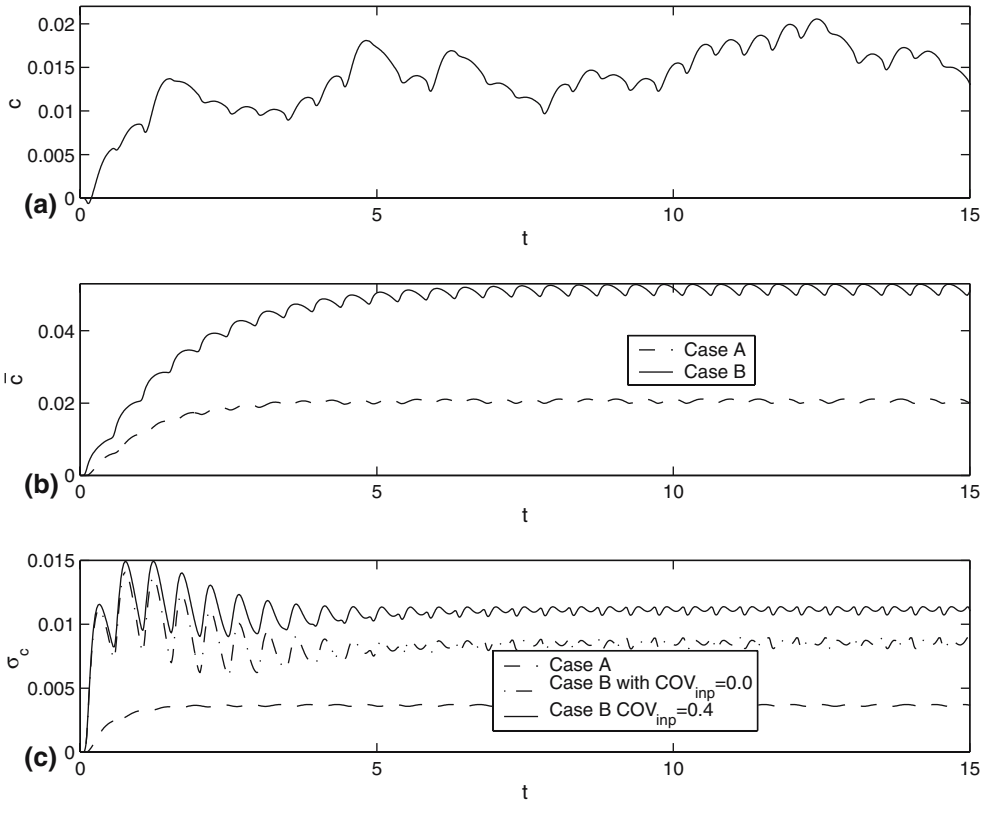

Fig. 12 The temporal behavior of concentration at location P_4 due to multiple random source pulses. **a** Break through curve of a single realization. **b** Comparison of mean concentration between Cases A and B. **c** Comparison of standard deviation of concentration between Cases A and B with deterministic source ($COV_{inp} = 0.0$) and random source ($COV_{inp} = 0.4$)

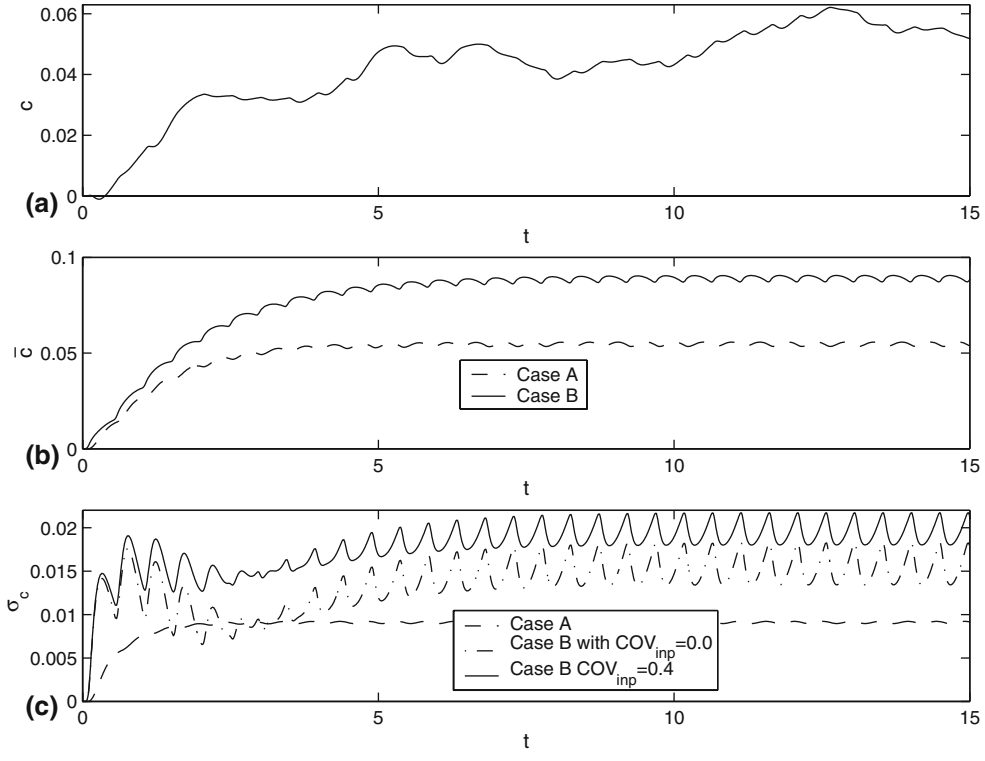

Fig. 13 The temporal behavior of concentration at location P_5 due to multiple random source pulses. **a** Break through curve of a single realization. **b** Comparison of mean concentration between Cases A and B. **c** Comparison of standard deviation of concentration between Cases A and B with deterministic source ($COV_{inp} = 0.0$) and random source ($COV_{inp} = 0.4$)

higher than the other locations away from the source (P_2, P_3, P_4 and P_5). The variation of temporal behavior of the standard deviation of concentration at different location for homogeneous and heterogeneous is mainly caused by the negative auto-covariance of concentration.

Table 2 The comparison of time averaged of mean concentration ($\bar{c}$) and coefficient of variation of concentration (COV_c) at large time for various test Cases A–F with deterministic source ($COV_{inp} = 0.0$) and random source ($COV_{inp} = 0.4$)

Location		A	B	C	D	E	F
P_1	$\bar{c}$	2.099	2.558	2.703	1.587	2.773	1.632
	COV_c for $COV_{inp} = 0.0$	0.0	0.429	0.451	0.455	0.448	0.452
	COV_c for $COV_{inp} = 0.4$	0.177	0.455	0.474	0.490	0.470	0.485
P_2	$\bar{c}$	0.230	0.181	0.141	0.092	0.272	0.176
	COV_c for $COV_{inp} = 0.0$	0.0	0.156	0.227	0.231	0.283	0.285
	COV_c for $COV_{inp} = 0.4$	0.176	0.209	0.261	0.270	0.308	0.314
P_3	$\bar{c}$	0.233	0.133	0.073	0.048	0.107	0.071
	COV_c for $COV_{inp} = 0.0$	0.0	0.208	0.106	0.111	0.140	0.144
	COV_c for $COV_{inp} = 0.4$	0.140	0.239	0.158	0.167	0.175	0.181
P_4	$\bar{c}$	0.021	0.052	0.068	0.045	0.117	0.077
	COV_c for $COV_{inp} = 0.0$	0.0	0.165	0.289	0.289	0.372	0.370
	COV_c for $COV_{inp} = 0.4$	0.177	0.216	0.315	0.319	0.391	0.391
P_5	$\bar{c}$	0.055	0.089	0.089	0.059	0.152	0.101
	COV_c for $COV_{inp} = 0.0$	0.0	0.172	0.255	0.254	0.345	0.342
	COV_c for $COV_{inp} = 0.4$	0.166	0.218	0.283	0.287	0.364	0.364

8 Conclusions

This paper illustrates a method for the probabilistic analysis of the concentration distribution in a 3-D heterogeneous porous media when the source condition is assumed to be a random process. The randomness in the source condition is limited to the amount of mass released at a fixed location with constant interval. The system uncertainty is due to the heterogeneity in the governing flow and transport parameters which are treated as random fields.

For a unit single source pulse the presence of uncertainty in the governing parameters cause the resulting response/impulse function to be stochastic in nature. This uncertainty in the concentration behavior (response function) is modeled using an efficient stochastic finite element method. A procedure developed here, which uses the numerically obtained response (Green) function to the case of multiple random source condition. The behavior of the stochastic response function has been studied for various parameters and coefficient of variation of random governing parameters.

The study indicates that the mean concentration is affected only by the uncertainty of the system parameters since the spatial random variation in the parameters cause the effective parameters (e.g. effective hydraulic conductivity, macrodispersivity) to differ from their mean values. The uncertainty associated with the temporal variation in the random source condition has no effect on the mean concentration. However, the standard deviation is affected by both randomness in source condition and system parameters and increases with increase in uncertainty of source condition. It is also noted that the comparative effects of randomness in the system parameters vis-a-vis the randomness in source condition are not similar at various locations in the domain.

The study can be extended in future considering improved approximation for random source conditions involving randomness in the source location and interval in the temporal occurrence of the event.

9 Appendix: mean and covariance of velocity and dispersion coefficient

Using the similar methodology presented for the transport problem (Sect. 4), the perturbation approach can also be applied on the flow Eq. 12, to obtain the mean and random perturbed components of the hydraulic head. In the case of the flow problem the random properties are only the hydraulic conductivities of the elements K_p, ($p = 1,2,..., N_k$) and hence the mean and the random component of the hydraulic head are expressed as,

$$\{\bar{h}\} = \left([\mathrm{I}] + \sum_{p=1}^{N_k} \sum_{q=1}^{N_k} [\bar{K}]^{-1} [K]^{(\mathrm{I})}_{K_p} [\bar{K}]^{-1} [K]^{(\mathrm{I})}_{K_q} \overline{K'_p K'_q} \right) \times [\bar{K}]^{-1} \{h_0\}, \tag{30}$$

$$\{h\}' = \sum_{p=1}^{N_k} \{h\}^{(\mathrm{I})}_{K_p} K'_p \quad \text{where } \{h\}^{\mathrm{I}}_{K_p} = -[\bar{K}]^{-1} [K]^{(\mathrm{I})}_{K_p} [\bar{K}]^{-1} \{h_0\}. \tag{31}$$

Using Eqs. 30 and 31 the mean and random component of seepage flux (q_{i_p}) are written as,

$$\bar{q}_{i_p} = -\frac{1}{N_G} \sum_{k=1}^{N_G} \left. \frac{\partial N_l(\mathbf{x})}{\partial x_i} \right|_{\mathbf{x}_k} \left(\bar{K}_p \bar{h}_l + \sum_{q=1}^{N_k} h^{(\mathrm{I})}_{l,K_q} \overline{K'_p K'_q} \right), \tag{32}$$

$$q'_{i_p} = -\sum_{q=1}^{N_k} \frac{1}{N_G} \sum_{k=1}^{N_G} \left. \frac{\partial N_l(\mathbf{x})}{\partial x_i} \right|_{\mathbf{x}_k} \left(\bar{h}_l \delta_{pq} + \bar{K}_p h^{(\mathrm{I})}_{l,K_q} \right) K'_q = \sum_{q=1}^{N_k} q^{(\mathrm{I})}_{i_p,K_q} K'_q. \tag{33}$$

From the above expression one can obtain the auto covariance of velocity and cross covariance with any other random properties (r'_j) using the auto covariance of hydraulic conductivity and cross covariance of hydraulic conductivity with r'_j, which may be given as34

$$\overline{q'_{i_{p_1}} q'_{j_{p_2}}} = \sum_{q_1=1}^{N_k} \sum_{q_2=1}^{N_k} q^{\mathrm{I}}_{i_{p_1},K_{q_1}} q^{\mathrm{I}}_{j_{p_2},K_{q_2}} \overline{K'_{q_1} K'_{q_2}} \quad \text{and}$$

$$\overline{q'_{i_p} r'_j} = \sum_{q=1}^{N_k} q^{\mathrm{I}}_{i_p,K_q} \overline{K'_q r'_j}. \tag{34}$$

$\bar{q}_{i_p}$ and q'_{i_p} are respectively the mean and the random component of the product $n_p v_{i_p}$ in the Eq. 7. The product $n_p D_{ij_p}$ can be written in terms of water flux,

$$n_p D_{ij_p} = \alpha_p \left((1-\epsilon) \frac{q_{i_p} q_{j_p}}{q_p} + \epsilon q_p \delta_{ij} \right) + n_p D_{m_p} \delta_{ij}. \tag{35}$$

The mean of the resultant seepage flux $\left(q_p = \left(\sum_{i=1}^{3} q_{i_p}^2 \right)^{1/2} \right)$ and its random component are expressed as,

$$\bar{q}_p = q_p + \frac{1}{q_p} \sum_{i=1}^{3} C_{q_{i_p} q_{j_p}} - \frac{1}{q_p^3} \sum_{i=1}^{3} \sum_{j=1}^{3} \bar{q}_{i_p} \bar{q}_{j_p} C_{q_{i_p} q_{j_p}}, \quad \text{and}$$

$$q'_p = \frac{1}{q_p} \sum_{i=1}^{3} \bar{q}_{i_p} q'_{i_p}. \tag{36}$$

The effective mean dispersion coefficient and its random component are obtained by using Eq. 3, along with the expression Eq. (36), which may be expressed as,

$$\begin{aligned} \overline{n_p D_{ij_p}} = & \left(\bar{\alpha}_p \left(\frac{\bar{q}_{i_p} \bar{q}_{j_p} + C_{q_{i_p} q_{j_p}}}{\bar{q}_p} \right. \right. \\ & \left. - \frac{\bar{q}_{i_p} C_{q_{j_p} q_p} + \bar{q}_{j_p} C_{q_{i_p} q_p}}{\bar{q}_p^2} + \frac{\bar{q}_{i_p} \bar{q}_{j_p} C_{q_p q_p}}{\bar{q}_p^3} \right) \\ & \left. + \frac{\bar{q}_{i_p} C_{q_{j_p} \alpha_p} + \bar{q}_{j_p} C_{q_{i_p} \alpha_p}}{\bar{q}_p} - \frac{\bar{q}_{i_p} \bar{q}_{j_p} C_{q_p \alpha_p}}{\bar{q}_p^2} \right) (1-\epsilon) \\ & + \epsilon (\bar{\alpha}_p \bar{q}_p + C_{q_p \alpha_p}) \delta_{ij} + \left(\bar{n}_p \bar{D}_{m_p} + C_{n_p D_{m_p}} \right) \delta_{ij} \end{aligned} \tag{37}$$

and

$$\begin{aligned} (n_p D_{ij_p})' = & \left(\bar{\alpha}_p \left(\frac{\bar{q}_{i_p} q'_{j_p} + \bar{q}_{j_p} q'_{i_p}}{\bar{q}_p} - \frac{\bar{q}_{i_p} \bar{q}_{j_p} q'_p}{\bar{q}_p^2} \right) + \alpha'_p \frac{\bar{q}_{i_p} \bar{q}_{j_p}}{\bar{v}_p} \right) (1-\epsilon) \\ & + \epsilon \left(\bar{\alpha}_p q'_p + \alpha'_p \bar{q}_p \right) \delta_{ij} + \left(\bar{n}_p D'_{m_p} + n'_p \bar{D}_{m_p} \right) \delta_{ij}. \end{aligned} \tag{38}$$

References

Bellin A, Saladin S, Rinaldo A (1992) Simulation of dispersion in heterogeneous porous formation: Statistics, first-order theories, convergence of computation. Water Resour Res 28:2211–2227

Bosma WJP, van der Zee SEATM (1995) Dispersion of continuously injected, nonlinear adsorbing solute in chemically or physically heterogeneous porous formation. J Contam Hydrol 18:181–198

Chaudhuri A, Chakraborty S (2006) Reliability of linear structures with parameter uncertainty under non-stationary earthquake. Struct Saf 28(3):231–246

Chaudhuri A, Sekhar M (2005a) Analytical solutions for macrodispersion in a 3D heterogeneous porous medium with random hydraulic conductivity and dispersivity. Transp Porous Media 58:217–241

Chaudhuri A, Sekhar M (2005b) Stochastic finite element method for probabilistic analysis of flow and transport in a 3-D heterogeneous porous formation. Water Resour Res 41, W09404. DOI:10.1029/2004WR003844

Cushman JH (1997) The physics of fluid in hierarchical porous media: angstroms to miles. Kluwer, Norwell

Dagan G (1989) Flow and transport in porous formations. Springer, Berlin Heidelberg New York

de Marsily (1986) Quantitative hydrology: groundwater hydrology for engineers. Academic, Orlando

Gao W, Chen JJ, Ma J, Liang ZT (2004) Dynamic response analysis of stochastic frame structures under nonstationary random excitation. AIAA J 42(9):1818–1822

Gelhar LW (1993) Stochastic subsurface hydrology. Prentice-Hall, Englewood Cliff

Hantush MH, Marino MA (1994) One-dimensional stochastic analysis in leaky aquifers subject to random leakage. Water Resour Res 30(2):549–558

Hassan AE (2001) Water flow and solute mass flux in heterogeneous porous formations with spatially random porosity. J Hydrol 242:1–25

Hassan AE, Cushman JH, Delleur JW (1999) A Monte Carlo assessment of Eulerian flow and transport perturbation models. Water Resour Res 34(5):1143–1163

Hu BX, Cushman JH, Deng FW (1997) Nonlocal reactive transport with physical, chemical and biological heterogeneity. Adv Water Resour 20:293–308

Huang H, Hu BH (2000) Nonlocal nonreactive transport in heterogeneous porous media with interregional mass diffusion. Water Resour Res 36(7):1665–1675

Kapoor V, Gelhar LW (1994) Transport in three-dimensionally heterogeneous aquifers, 2. Prediction and observations of concentration fluctuations. Water Resour Res 30(6):1789–1801

Li L, Graham WD (1999) Stochastic analysis of solute transport in heterogeneous aquifers subject to spatiotemporal random recharge. Water Resour Res 35(4):953–971

Melching CS, Yoon CG (1996) Key sources of uncertainty in QUAL2E model of Passaic River. J Water Resour Plann Manage 122(2):105–113

Osnes H, Langtangen HP (1998) An efficient probabilistic finite element method for stochastic groundwater flow. Adv Water Resour 22(2):185–195

Rowe RK, Booker JR (1986) A finite layer technique for calculating three-dimensional pollutant migration in soil. Geotechnique 36(2):205–214

Spanos PD, Ghanem R (1989) Stochastic finite element expansion for random media. ASCE Eng Mech 115(5):1035–1053

Subbarao VVR, Mujumdar PP, Ghosh S (2004) Risk evaluation in water quality management of a river system. J Water Resour Plann Manage 130(5):411–423

Tang DH, Pinder GF (1979) Analysis of mass transport with uncertain physical parameters. Water Resour Res 15(5):1147–1153

Vanmarcke EH (1983) Random field analysis and synthesis. MIT Press, Cambridge

Wang PP, Zheng C (2005) Contaminant transport models under random sources. Ground Water 43(3):423–433